

Recovery of Systematic Biases in Laser Altimeters Using Natural Surfaces

Sagi Filin

Department of Civil and Environmental Engineering and Geodetic Science, The Ohio State University
Department of Geodesy, Faculty of Civil Engineering and Geosciences, Delft University of Technology, The Netherlands*
s.filin@citg.tudelft.nl

Commision 3, Working Group 3

KEY WORDS: Laser Altimetry, Error model, Calibration

ABSTRACT

Elements of accuracy of LIDAR systems and the corrections of systematic errors have received growing attention in recent years. The expected level of accuracy and the additional processing that is needed for making the raw data ready to use are affected directly by the systematic errors in the laser data. It is evident that calibration of the LIDAR system, both laboratory and in-flight, are mandatory to alleviate these deficiencies. This paper presents an error recovery model that is based on modeling the system errors and on defining adequate control information. The association of the observations and control information, and configurations that enhance the reliability of the recovered parameters, are also studied here in detail.

1 Introduction

Laser altimetry has emerged in recent years as a leading technology for capturing data of physical surfaces. Properties like the relatively high accuracy, the expected short turnout time, and a detailed and almost ready-made digital surface model (DSM) that is generated by the system, ensure the growing interest in this technology. While a detailed coverage of the surveyed surface is achieved by an increased system sampling rate and thereby the point density, achieving the expected level of accuracy and ensuring a short turnout time depend in large on maintaining the potential quality of the data. A major factor that affects the data quality is the existence, and thus removal, of the systematic errors in the data.

A growing number of publications in recent years report the existence of systematic errors in the laser data and their effect on the accuracy and on the processing of laser data. For example, Huising and Gomes Pereira (1998) report about systematic errors of 20 cm in elevation and of several meters in position between overlapping laser strips, Crombaghs et al. (2000) and Vosselman and Mass (2001) identify systematic trends between overlapping strips, and Hofton et al. (2000) report about identifying systematic errors in NASA's Scanning Lidar Imager of Canopies by Echo Recovery (SLICER) (Blair et al., 1994). The systematic errors have several effects on the laser data. Clearly they degrade the accuracy of the geolocation of the laser footprint. Furthermore, they distort the surface that is reconstructed by the laser data in several ways, some of them linear (shifts and rotations) but others not. One consequence of the distortions is that surveyed objects in the overlapping areas of different laser swaths may not coincide. Corrections then require a relatively long preprocessing time that, in turn, increases the turnout time. Reducing the effect of such errors requires pre-flight system calibration (Krabill et al., 1995; Ridgway et al., 1997) as well as in-flight calibration.

To eliminate the effect of the systematic errors, several procedures have been proposed so far. One group can be categorized as data driven. The motivation is to correct the laser points by transforming them so that the difference be-

tween their values and the reference control information is minimized, namely,

$$\| (x_w, y_w, z_w) - T(x_l, y_l, z_l) \| = \min \quad (1)$$

where the subscripts l, w denote laser and world respectively, and $\| \cdot \|$ is the l_2 norm. Mostly, the corrections are modeled by means of the similarity transformation (Postolov et al., 1999; Crombaghs et al., 2000; Mass, 2000), which involves translations and rotations of the laser points. Another approach is based on recovering the systematic *system* errors. Several authors report recovering the errors by conducting different flight patterns over flat locally horizontal surfaces and "flattening" the surface as a function of the systematic errors (Vaughn et al., 1996; Ridgway et al., 1997; Hofton et al., 2000). Others (e.g., Kilian et al., 1996) base their calibration procedure on control, height, and tie points, in a fashion similar to photogrammetric block adjustment, or propose to reconstruct the elevation model (Burman, 2000) around distinct landmarks to tie the overlapping strips.

The correction of laser points by means of a linear transformation focuses on the effect of the systematic errors but not on their causes. This may not always be appropriate; an analysis of the similarity transformation (Filin et al., 2001) reveals that not all error effects can be modeled, and thus removed, by this transformation. Therefore, some accuracy may be lost, and more complicated algorithms may be needed. Calibration approaches that are based on flying over flat locally horizontal surfaces have their own limitations. For one, planar surfaces are not always available, and furthermore they cannot model the effects of several error sources, like the positional offsets. In general, the concept of control information has not been fully explored. The information carried by laser points is rather limited as it consists of the 3-D coordinates of the laser point without any additional information such as radiometric intensity. The laser points position is, however, distorted by the errors, and identifying the footprint location (the actual location of the laser point) is practically impossible. Flattening the reconstructed surface is one way to circumvent the lack of information and identifying distinct control landmarks is another one. The limitations are, however, clear; both approaches require the existence of such objects, and in the case of distinct control features, they also depend on the altimeter sampling rate.

*The research was conducted while the author was with the department of Civil and Environmental Engineering and Geodetic Science at The Ohio State University. The author is currently with the Department of Geodesy at Delft University of Technology.

The strategy presented in this paper is based on utilizing natural and man-made surfaces to recover the calibration parameters. The approach has several advantages. It is relatively simple to apply even in areas that traditionally are not considered favorable for calibration, and does not require control points or flat locally horizontal surfaces. The algorithm also simplifies the sought correspondence between the laser points and ground control information and offers a more general solution that does not depend on well-defined control landmarks. In addition, the formulation enables one to model the outcome of different systematic effects and to analyze the preconditions for their recovery. Thereby, an analytical look into the potential recovery of different biases is made possible.

The paper is organized as follows. The next section presents the approach for the error recovery, it consists of the error modeling and the recovery model. Following is an analysis of the model properties, and of elements that enhance the reliability of the recovered parameters. Results and discussion conclude the presentation.

2 Error recovery

In-flight calibration of laser systems is complicated. The error model involves the intrinsic errors of each system component as well as errors that are a consequence of their integration. A detailed error model is provided by Schenk (2001), but it is clear that the error model is not yet fully understood. In addition, the calibration procedure involves more than the formulation of an analytical error model. System calibration belongs, in general, to the class of inverse problems. For many of them knowledge about the relation between the target and domain data (dubbed here correspondence) is assumed to be known, so the focus is on solving the inverse problem. With laser mapping, however, it is impossible to know the exact footprint location, and thus establishing a relation between the domain (a laser point) and the target data (the footprint). Solving the inverse problem requires to find first the correspondence by some method. This problem indicates that the calibration is in fact a strategy rather than a formulation of the calibration equation. The geometric realization of the data acquisition system poses another problem. In general, from each firing point only one beam is being transmitted and therefore leaves no intrinsic redundancy. One potential effect of this configuration is an increased correlation of the calibration parameters that implies that not all the systematic errors may be recovered independently. Therefore, another question is which errors can be recovered and how to solve for them.

The approach taken here is focused on the geolocation of the laser footprint. The goal is finding the best geolocation of the laser points in terms of minimizing the l_2 norm of the differences between the laser point coordinates and the ground. Two spatial relations are involved in this modeling – the laser geolocation equation and the surface model. The geolocation and the error modeling are presented first.

2.1 Footprint geolocation and error modeling

The laser geolocation equation models the incorporation of the different components of a laser altimeter system by means of the transformations between the different reference frames. The form is well established (see e.g., Vaughn et al., 1996; Schenk, 2001) and is given in eq. 2.

$$\begin{bmatrix} x_l \\ y_l \\ z_l \end{bmatrix} = \begin{bmatrix} X_0 \\ Y_0 \\ Z_0 \end{bmatrix} + R_W R_G R_{INS} \left(\begin{bmatrix} \delta_x \\ \delta_y \\ \delta_z \end{bmatrix} + R_m R_s \begin{bmatrix} 0 \\ 0 \\ -\rho \end{bmatrix} \right) \quad (2)$$

where:

- x_l, y_l, z_l – location of the footprint in WGS-84 geocentric coordinate system.
- X_0, Y_0, Z_0 – location of the phase center of the GPS receiver.
- R_W – rotation from the local ellipsoidal system into the WGS-84 geocentric reference frame.
- R_G – rotation from reference system defined by the local vertical, to the ellipsoidal reference frame.
- R_{INS} – rotation from body reference frame to reference frame defined by local vertical. Rotations are defined according to the INS angles.
- $\delta_x, \delta_y, \delta_z$ – offset vector between the phase center of the GPS antenna and laser firing point, defined by the body frame.
- R_m – the mounting bias, which designate rotation between the altimeter and the body frame.
- R_s – rotation between laser beam and laser system defined by scanning angles.
- ρ – range measured by laser system.

The systematic errors are analytically modeled by their effect on the geolocation equation. A standard error model is yet to be set, and the literature shows that the type of modeled errors vary from one author to another. Schenk (2001) lists as many as six potential groups of error sources. They include (i) ranging errors, (ii) scan angle errors that consist of an error in the swath angle, and in the determination of the scan plane, (iii) mounting errors that consist of errors in determining the alignment between altimeter and the INS, and of an error in the determination of the offset between the phase center of the GPS antenna and the laser system, (iv) INS errors (v) position errors, and (vi) timing errors. Some of these errors may be fixed during the flight mission, while others may vary over time or as a function of position. Identifying the effect of each error source is not always possible and under given conditions several groups of the errors can have similar effects. A detailed study of the effects and conditions for the recovery of the errors can be found in Schenk (2001) and Filin (2001). In this paper, two error sources that are considered to have the major effect on the geolocation (see e.g., Vaughn et al., 1996; Hofton et al., 2000; Ridgway et al., 1997) are studied. They consist of the mounting bias and the range bias. The effect of the mounting bias was modeled already in eq. 2, and the range bias models a constant offset in the range determination. An interesting effect of the range bias is that it may result in a nonlinear surface deformation. The mounting bias can be approximated, in general, by measurements prior to the mission and can be treated as composed of a measured part and an unknown part (thus modeled as $\Delta R_m R_m$, with ΔR_m as the unknown part). For simplicity it is modeled here as a single entity with the measured part considered as a first

approximation. The modified geolocation equation with the two error sources, and the effect of the random errors is given in eq. 3

$$\begin{bmatrix} x_l \\ y_l \\ z_l \end{bmatrix} = \begin{bmatrix} X_0 \\ Y_0 \\ Z_0 \end{bmatrix} + R_W R_G R_{INS} \left(\begin{bmatrix} \delta_x \\ \delta_y \\ \delta_z \end{bmatrix} + R_m R_s \begin{bmatrix} 0 \\ 0 \\ -(\rho + \delta\rho) \end{bmatrix} \right) + \begin{bmatrix} \bar{e}_x \\ \bar{e}_y \\ \bar{e}_z \end{bmatrix} \quad (3)$$

with $\delta\rho$ – the range bias, $\bar{e}_x, \bar{e}_y, \bar{e}_z$ – and the random errors for the x, y , and z coordinates respectively. The mounting bias can be described by the three Euler angles, and, together with the range bias, there are four unknowns. Performing the following derivations in a geocentric reference frame does not contribute much to the problem formulation. As the term $R_W R_G$ can be approximated by a constant for a relatively large surface size, it is multiplied out and the reference frame is also shifted to the surface elevation, thereby forming a local reference frame.

2.2 Error recovery model

To recover the systematic biases the surface is introduced as a constraint. A general expression for a surface is given in eq. 4

$$f(x, y, z) = 0 \quad (4)$$

The footprint coordinates can be viewed as a vector-valued function g of the observations – Y , the systematic errors – Ξ , and the random errors – \bar{e} that is written in the following form – $\mathbf{1} = g(Y, \Xi, \bar{e})$, with $\mathbf{1} = [x_l, y_l, z_l]^T$. Consequently, the following relation can be written

$$f(x_l, y_l, z_l) = h(Y, \Xi, \bar{e}) = 0 \quad (5)$$

with h the implicit representation of the surface as a function of the observations, and the systematic and the random errors. The obvious target function is minimizing the l_2 -norm of the residual vector, which also has the property of providing the best linear uniformly unbiased estimate for the parameters.

An explicit form of the surface function is, in general, not known. It is more realistic to assume that the surface consists of a set of surface elements, each with its analytical form. The current modeling assumes that the surface can be represented by a set of a planar surfaces

$$s_1 x + s_2 y + s_3 z + s_4 = 0 \quad (6)$$

although any other surface model can be used. In this form $\mathbf{s} = [s_1, s_2, s_3]$ is the surface normal direction and s_4 is the intercept point. The surface parameters are considered here to be known a priori. Incorporation of the surface constraint and geolocation equation (eq. 3) is given in eq. 7

$$\mathbf{s} \left[\begin{bmatrix} X_0 \\ Y_0 \\ Z_0 \end{bmatrix} + R_{INS} \left(\begin{bmatrix} \delta_x \\ \delta_y \\ \delta_z \end{bmatrix} + R_m R_s \begin{bmatrix} 0 \\ 0 \\ -(\rho + \delta\rho) \end{bmatrix} \right) \right] + \mathbf{s} \begin{bmatrix} \bar{e}_x \\ \bar{e}_y \\ \bar{e}_z \end{bmatrix} + s_4 = 0 \quad (7)$$

The relation in eq. 7 is the scalar product between the representation of the laser point in homogeneous coordinates and the surface, namely,

$$\bar{\mathbf{s}} \cdot \bar{\mathbf{1}} = 0 \quad (8)$$

with $\bar{\mathbf{s}} = [s_1 \ s_2 \ s_3 \ s_4]$ and $\bar{\mathbf{1}} = [x_l \ y_l \ z_l \ 1]$.

Linearization of this form is given in eq. 9. First approximations can either be set to zero or to the prior information values if ones exist.

$$\bar{\mathbf{s}} \cdot \bar{\mathbf{1}} = (\mathbf{s} R_{INS} \mathbf{U})_{1 \times 3} \begin{bmatrix} \kappa \\ \phi \\ \omega \end{bmatrix}_{3 \times 1} + (\mathbf{s} R_{INS} R_s)_{1 \times 3} \begin{bmatrix} 0 \\ 0 \\ \delta\rho \end{bmatrix} + \mathbf{s} \bar{\mathbf{e}} \quad (9)$$

with ω, ϕ, κ , the bias angles along the x, y , and z -axes, respectively; $\bar{\mathbf{1}}$, the approximation for the geolocation of the laser point (according to the current knowledge of the biases), and $\mathbf{U}_{3 \times 3}$ a matrix of the form

$$\mathbf{U} = \begin{bmatrix} -v & w & 0 \\ u & 0 & -w \\ 0 & -u & v \end{bmatrix} \quad (10)$$

where

$$\begin{bmatrix} u \\ v \\ w \end{bmatrix} = R_s \begin{bmatrix} 0 \\ 0 \\ -\rho \end{bmatrix} \quad (11)$$

Notice that each laser point contributes one equation. The model parameters are recovered via the Gauss-Helmert model,

$$w_n = A_{n \times m} \xi_m + B_{n \times 3n} e_{3n} \quad , \quad e \sim \{0, \sigma_0^2 P^{-1}\} \quad (12)$$

with w , the transformed observation vector; A , the coefficient matrix; B , the conditions matrix; ξ , the vector of unknowns; e , the observational noise; P , the weight matrix; σ_0^2 , the variance component; n , the number of laser points; and m , the number of unknowns. The least-squares criterion results in

$$\hat{\xi} = (A^T (B P^{-1} B^T)^{-1} A)^{-1} A^T (B P^{-1} B^T)^{-1} w \quad (13)$$

with:

$$\hat{D}\{\hat{\xi}\} = \hat{\sigma}_0^2 (A^T (B P^{-1} B^T)^{-1} A)^{-1} \quad (14)$$

$$\hat{\sigma}_0^2 = \frac{(B \tilde{e})^T (B P^{-1} B^T)^{-1} (B \tilde{e})}{n - m} \quad , \quad B \tilde{e} = w - A \hat{\xi} \quad (15)$$

Notice that with this formulation the essence of the problem is modeled; the 3-D laser points and the surface are constrained. Furthermore, an explicit surface model incorporates additional information about the terrain, such as slopes, into the calibration model. In addition, with this formulation, no

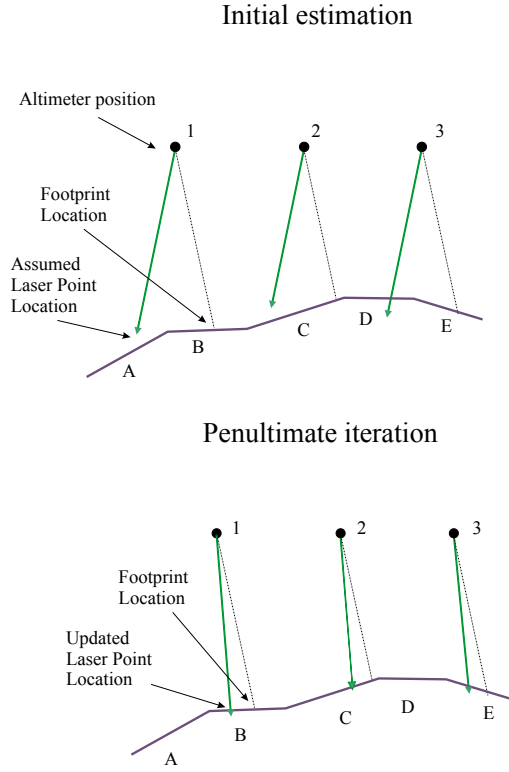


Figure 1: The iteration process – second level

restriction on the surface type, e.g., flat locally horizontal surfaces, is needed. The approach is also independent of the altimeter system sampling rate. Instead of focusing on the reconstructed surface the model concerns the laser points themselves. Therefore, distinct landmarks such as breaklines and corners are not needed; the focus, here, is on minimizing the distances between the points to the ground, the density of the laser points is, therefore, not as significant.

Extension of this model to accommodate for other types of errors can be carried out by modifying the laser geolocation equation. The extension however does not mean that all the errors are recoverable; further analysis of recoverability conditions is required.

3 Model Analysis

The construction of the error recovery model enables one to study of several aspects in greater detail. One aspect is establishing a more general model for the correspondence between the laser points and the surface. Another is analyzing the configurations that enhance the reliability of the parameter recovery.

3.1 Detection of the correspondence

The proposed model simplifies significantly the detection of the correspondence between the laser points and the control information; the association here is between the laser points and the surface elements that contain the footprint. That is a subtle but important difference between association of the laser points and their corresponding ground position. The current association is less restrictive insofar as it does not require well-defined 3-D landmarks for calibrating the system. In fact, laser points that fall “inside” ordinary surfaces (i.e.,

not “on” or near breaklines) are as good or even better than any other points in terms of accuracy.

Nevertheless, simplifying the correspondence does not guarantee that the initial association between the laser points, before being corrected for the systematic errors, and the surface elements is indeed correct. It is still possible that the laser points will fall inside wrong surface elements; see, for example the initial estimations in Figure 1. Here, point 1 is initially associated with surface element A instead of surface element B, point 2 is correctly associated with surface element C, and point 3 is, again, wrongly associated with surface element D instead of E. The approach presented here solves this problem by an iterative convergence to the true solution. The approach resembles the concepts of deformable templates, and the Iterative Closest Point (ICP) algorithm (Besl and McKay, 1992). The algorithm works as follows. Correspondence is established by the initial location of the laser points; surface parameters are then derived for each laser point. After construction of the observation and condition matrices and the transformed observation vector, the parameters are estimated by the Gauss-Helmert model (eq. 12). In the following iteration the correspondence is updated according to the modified position of the laser point, and the computation of the systematic errors repeats itself. Convergence is reached when the errors are not updated further, which occurs when the points fall on the true surfaces, see the penultimate iteration in figure 1. The algorithm below summarizes the steps that are taken

1. initialize $\hat{\Xi}$ and $\hat{\xi}$
2. **while** $\hat{\xi} \neq 0$, **do**
3. **for each** laser point, l_j , **do**
4. compute the incident point –
 $\{x_j, y_j, z_j\} = g(l_j, \hat{\Xi}_i)$
5. compute $s_j = f(x_j, y_j, z_j)$
6. Solve for $\hat{\xi}_i$ using eq. 13
7. $\hat{\Xi} = \hat{\Xi} + \hat{\xi}$
8. **endwhile**
9. declare convergence,

Problems may be encountered with points near breaklines between surfaces with a relatively big height discontinuity. The large differences are likely to bias the solution to compensate for the differences. This problem can be circumvented either by robust estimation techniques, or by removing error prone points prior to the adjustment, for example, by evaluating the homogeneity of points’ neighborhood.

3.2 Configuration and Reliability

The analytical error recovery model that was derived in Section 2.2 provides a closed form that incorporates the laser points, the errors and the surface parameters. It enables the analysis of the elements that influence the recovery of the systematic biases and the study of configurations that provide a better and more reliable estimation of the systematic errors. The analysis begins with the linearized form of the observation equations given in equation 9. An explicit form is given by

$$w = -(c_2\omega_i + c_3)\delta\rho + (-c_1v + c_2u)\kappa + (c_1w - c_3u)\phi + (-c_2w + c_3v)\omega + s_1\bar{e}_x + s_2\bar{e}_y + s_3\bar{e}_z \quad (16)$$

with $\mathbf{c} := [c_1 \ c_2 \ c_3] = \mathbf{s}R_{INS}$. The vector \mathbf{c} can be viewed as a modified surface slope determined as a function of the aircraft attitude and the surface slope. The values for u, v, w are defined by eq. 11.

The form in equation 16 is general and can be applied to different types of scanning systems. We analyze it with respect to a linear scanner configuration which is widely used in laser mapping. For a linear scanning system the rotation matrix R_s is given by $R_s = R_x(\omega_i)$. Consequently the laser beam pointing direction can be approximated by $[u \ v \ w] \approx [0 \ -\omega_i \rho \ -\rho]$. Equation 16 can be written then as

$$w = -(c_2\omega_i + c_3)\delta\rho + c_1\omega_i\rho\kappa - c_1\rho\phi + (c_2 + c_3\omega_i)\rho\omega + s_1\bar{e}_x + s_2\bar{e}_y + s_3\bar{e}_z \quad (17)$$

The recovery of the calibration parameters depends in large on the modified surface slope and on the scanning angle; the positional dependency shows itself only through the range, but this effect is not big. The dependency on the angular quantities vary, however, from one parameter to another. Equation 17 shows that the pitch bias, ϕ , depends on the modified slope c_1 along the flight direction while the coefficients for the mounting bias in the roll direction, ω_i , depends on the modified surface slope across the flight direction. This coefficient can be viewed as the sum of the surface tilt across the flight direction and the scanner pointing angle. The coefficient for the heading bias, κ , depends on the product of the slope along the flying direction and the pointing angle and is expected to be smaller by an order of magnitude compared to the other two. The coefficient for the range bias can be regarded fixed up to variations as a function of surface slope along the flying direction and the scanning angle.

To recover the four biases simultaneously, the observation matrix, A , should have neither zero nor linear dependent columns. Equation 17 shows that zero columns can occur if the modified surface slopes in the roll direction c_1 is constantly equal to zero, namely a zero slope along the flying direction. It is very unlikely to encounter situations in which the roll bias coefficients are all zero or close to zero, unless c_2 and ω_i constantly cancel one another. The scanner angle contribution indicates that no slope variation across the flying direction is needed to recover the roll bias. Notice also that the slope variations can be achieved by aircraft maneuvers, so theoretically the recovery of the four parameters can be performed by flying over a flat horizontal surface. This is however not an optimal configuration because maneuvers may introduce additional errors that will degrade the quality of the estimated parameters. It is, therefore, recommended to recover the errors by using observations taken over sloping surfaces. Configurations that result in a linear dependency or in columns that are almost similar are possible to construct. One example, is using observations in which the value of the scan angle, ω_i is almost fixed. With this configuration the coefficients for κ and ϕ are similar. Another configuration that may result in similar columns occurs when calibrating the system over a single surface or surfaces with almost the same slope. Under such configuration high similarity is expected between the range and the pitch bias coefficients, and if c_2 is equal to zero, also between the heading and the roll bias. It is therefore recommended to use observations from

Conf.	Slope		Cond. Number	$tr\{N^{-1}\}$
	s_1	s_2		
I	0.01	0	236758.035	243.1
	-0.01	0		
II	0.1	0	13834.425	10.3
	0.2	0		
III	-0.1	0	2309	2.4
	0.1	0		
IV	-0.15	0	1050	1.1
	0.15	0		
V	-0.2	0	587	0.6
	0.2	0		
VI	-0.2	0.1	580	0.6
	0.2	-0.1		
VII	-0.2	0.1	650	0.6
	0.2	0.1		

Table 1: Effect of slope distribution

the two sides of the swath and to use surface elements with different slopes.

Configurations that enhance the reliability of the recovered parameters should minimize the trace of the dispersion matrix

$$tr\{D\{\hat{\xi}\}\} = \min \quad (18)$$

and results, in general, in a relatively small condition number and small correlation between the estimated parameter. The term configuration refers here to the slopes of the surface rather than to their spatial organization. Big surface slopes, and surface slopes in different directions have the effect of increasing the diagonal elements of the normal equations while reducing the off diagonal ones. Thus, smaller correlations and a smaller trace can be achieved this way.

The effect of different surface configurations is demonstrated in Table 1. The configurations are analyzed by the conditions number and by the trace of the cofactor matrix, $N^{-1} := (A^T(BP^{-1}B^T)^{-1}A)^{-1}$. With the first configuration the errors are recovered by flying over a surface with very mild slopes (one percent). The condition number is large and so is the trace of the cofactor matrix; the results are therefore less reliable. With the second configuration the errors are recovered by flying over surfaces with relatively big slopes, but ones that are pointing in the same direction. Comparing the results to those obtained by the third configuration demonstrates the effect of using surfaces that point in opposite directions. The trace of the cofactor matrix for configuration III is five times smaller than the one for configuration II, even though the surface slopes in configuration II are bigger. Configurations III-V show the effect of using steeper slopes. As can be seen, the trace decreases from 2.4 to 0.6 as the slopes change from 10 percent to 20 percent. In general, steeper slopes are preferable than smaller ones, however, the rang-

1.00	0.94	-0.08	0.08
0.94	1.00	-0.08	0.08
-0.08	-0.08	1.00	-0.94
0.08	0.08	-0.94	1.00

Table 2: Correlation matrix for configuration II, surface slopes pointing in the same direction

1.00	-0.10	-0.08	0.02
-0.10	1.00	-0.02	0.09
-0.08	-0.02	1.00	-0.04
0.02	0.09	-0.04	1.00

Table 3: Correlation matrix for configuration III, surface slopes pointing in positive and negative directions

ing accuracy decreases as a function of the slope increase, so the effect of steeper slopes is balanced by smaller weights. Configuration VI and VII show that surface slopes across the flight direction do not contribute to the quality of parameter estimation. The effect of the estimation of the κ angle on the condition number and the trace was evaluated in regards to configuration III. When recovering only the three parameters (assuming no bias in the heading direction) the condition number was reduced to 25 and the trace to 0.4. Eliminating other angular biases did not change much the original values.

The effect of the pointing direction of the surface slopes on the parameters correlation is demonstrated with respect to configurations II and III. Tables 2 and 3 list the correlation matrices of the estimated parameters for these two configurations. The order of parameters is - the range, the pitch, the roll, and the heading biases. The results show that the use of surfaces that point in positive and negative directions has also the effect of reducing the correlation, and thus making the recovery of each systematic error almost independent. Notice also that the high correlation in configuration II is between the range and the pitch bias and the heading and the roll bias. This type of correlation was anticipated when calibrating the system over surfaces with similar slopes (see the discussion above about configurations that result in high similarity between columns). The results show that even when variations in the surface slope are significant (but in the same direction) the similarity between the coefficients of the different parameters is high.

4 Discussion and results

The results of the analysis show that recovering the systematic error of LIDAR system is a manageable task, and one that can result in reliable estimates. The results show that by fairly simple means, like surfaces pointing in different directions solutions with a low condition number, and low correlation can be generated. Utilizing natural surfaces or man-made objects to resolve the systematic errors make this formulation advantageous to the existing methods as it neither limits the solution to flat surfaces nor requires distinct control features. Notice that the need for preliminary knowledge about the correspondence between laser points and the ground is removed; the proposed formulation solves for the calibration parameters and the correspondence simultaneously. In addition, with this model the solution to the correspondence problem is an in-

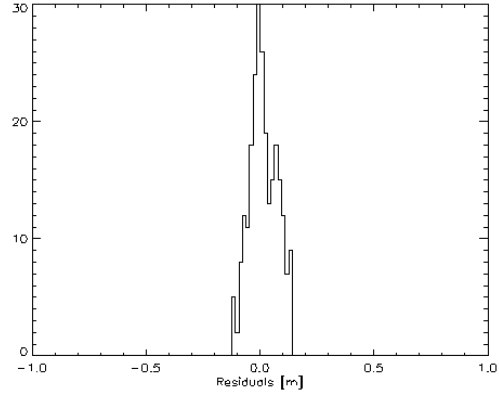


Figure 2: Frequency of residuals after removal of systematic errors

tegral part of the calibration model; no additional algorithms are needed to solve this part.

Experiments with the recoverability of the potential error sources shows that solutions with a minimum correlation and small variance can be achieved. The approach was applied to recover the calibration parameters of the NSF-SOAR (National Science Foundation Support Office for Aerogeophysical Research) laser altimetry system. The NSF-SOAR system is a unique suite of geophysical, mapping and navigational instruments, mounted in a ski-equipped aircraft. The system was flown in Antarctica to map surface elevation changes on the West Antarctica Ice Shelf (WAIS) ice streams (Spikes et al., 1999). The calibration of the NSF-SOAR laser system posed a challenge for existing calibration approaches since the whole mission was performed in the interior of the WAIS where neither flat surfaces nor distinct features were available. The profiling configuration also meant a relatively sparse sampling – one point per eight meters – and the comparison of a two dimensional object to a three dimensional one. Ground control information was available from snowmobile-mounted GPS surveys that was conducted along the skiways and their surroundings. Control surfaces were formed by a triangulation of the points, and planar surface parameters were computed using plane fitting. The site was overflowed several times including flights with constant attitude as well as with pitch or roll maneuvers. Data from flight segments that contributed to achieving the optimal configuration were used as observations. The parameters were recovered in a fairly high level of accuracy. Figure 2 presents the residual distribution after the system calibration. Evaluating the statistical characteristics shows that $\hat{\sigma}_0 = 0.06\text{m}$, the condition number for this calibration configuration is $C = 800$, and the highest correlation is 30 percent and the others are less than ten. These values validate the analysis in Section 3.2 and show that solutions with small variance and low correlation can be achieved even under less than optimal conditions.

5 Concluding remarks

This research studied the calibration of a laser altimeter system. An analysis of the data characteristics and the data acquisition concept has indicated a need for a model that is different from the traditional data registration concepts, e.g.,

the ones applied in photogrammetry. It was identified that the two prevailing problems are the nonredundant determination of laser points and the unknown correspondence between laser points and the spot they illuminate on the ground.

By analyzing the properties of the proposed method, it has been demonstrated that moderate slopes are sufficient to generate reliable solutions. The only requirement consists in having the surface elements oriented in different directions. The compelling conclusion is that natural terrain will yield results that are accurate and reliable.

Acknowledgment

The author would like to acknowledge Dr. Bea Csathó for making the NSF-SOAR data available and for her help in processing the data. This work was funded in part by the National Science Foundation grant OPP- 9615114.

REFERENCES

- Besl, P. J. and N. D. McKay (1992). A method for registration of 3-D shapes. *IEEE Trans. on PAMI*, **14**(2): 239–256.
- Blair, B., B. Coyle, J. L. Bufton and D. Harding (1994). Optimization of an Airborne Laser Altimeter for Remote Sensing of Vegetation and Tree Canopy. *Proceedings of IEEE*, 939–941.
- Burman, H. (2000). Adjustment of laser scanner data for correction of orientation errors. *International Archives of Photogrammetry and Remote Sensing*, **33**(B3/1): 125–132.
- Crombaghs, M., E. De Min and R. Bruegelmann (2000). On the Adjustment of Overlapping Strips of Laser Altimeter Height Data. *International Archives of Photogrammetry and Remote Sensing*, **33**(B3/1): 230–237.
- Filin, S. and B. Csathó (1999). A Novel Approach for Calibration of Satellites Laser Altimeters. *International Archives of Photogrammetry and Remote Sensing*, **32**(3–W14): 47–54.
- Filin, S., (2001), Calibration of spaceborne and airborne laser altimeters using natural surfaces. PhD Dissertation Department of Civil and Environmental Engineering and Geodetic Science, the Ohio-State University, Columbus, OH. To be published as a report in Geodetic Science and Surveying
- Filin, S., Csathó, B., Schenk T., (2001), An Analytical Model for In-flight Calibration of Laser Altimeter Systems Using Natural Surfaces, Proceedings of the Annual Conference of the American Society of Photogrammetry and Remote Sensing (ASPRS), St. Louis MS., published on CD-ROM.
- Hofton, M., B. Blair, J. B. Minster, J. R. Ridgway, N. Williams, J. L. Bufton and D. L. Rabine (2000). An Airborne Laser Altimetry Survey of Long Valley, California. *Int. J. Remote Sensing* **21**(12): 2413–2437.
- Huising, E. J. and L. M. Gomes Pereira (1998). Errors and accuracy estimates of laser data acquired by various laser scanning systems for topographic applications. *ISPRS J. of Photogrammetry and Remote Sensing*, **53**(5): 245–261.
- Kilian, J., N. Haala and M. English (1996). Capture of Elevation of Airborne Laser Scanner Data. *International Archives of Photogrammetry and Remote Sensing*, **31**(B3): 383–388.
- Krabill, W. B., R. H. Thomas, C. F. Martin, R. N. Swift and E. B. Frederick (1995). Accuracy of Airborne Laser Altimetry over the Greenland Ice Sheet. *Int. J. Remote Sensing*, **16**(7): 1211–1222.
- Maas, H. G. (2000). Least-Squares Matching with Airborne Laserscanning Data in a TIN Structure. *International Archives of Photogrammetry and Remote Sensing*, **33**(B3/1): 548–555.
- Postolov, Y., A. Krupnik and K. McIntosh (1999). Registration of airborne laser data to surface generated by photogrammetric means. *International Archives of Photogrammetry and Remote Sensing*, **32**(3–W14): 95–100.
- Ridgway, J. R., J. B. Minster, N. Williams, J. L. Bufton and W. B. Krabill. 1997. Airborne laser altimeter survey of Long Valley California. *Int. J. Geophys.*, **131**, 267–280.
- Schenk, T. (2001). Modeling and analyzing systematic errors of airborne laser scanners. *Technical Notes in Photogrammetry* No. 19, Department of Civil and Environmental Engineering and Geodetic Science, The Ohio State University, Columbus, OH., 40 pages.
- Spikes, B., B. Csathó and I. Whillans (1999). Airborne laser profiling of Antarctic ice streams for change detection. *International Archives of Photogrammetry and Remote Sensing*, **32**(3–W14): 169–175.
- Vaughn, C. R., J. L. Bufton, W. B. Krabill and D. L. Rabine (1996). Georeferencing of Airborne Laser Altimeter Measurements. *Int. J. Remote Sensing*, **17**(11): 2185–2200.
- Vosselman G., and Maas, H. G. (2001). Adjustment and filtering of raw laser altimetry data. In *Proceeding of OEEPE workshop on Airborne laser scanning and interferometric SAR for detailed digital elevation model.*, Stockholm, Sweden.